



Cite this: DOI: 10.1039/d5fb00384a

Sustainable biofilm control using lactic acid bacteria to disrupt quorum sensing in foodborne pathogens

Dimitra Kostoglou, Alexandra Vlachopoulou, Georgios Vafeiadis
and Efstathios Giaouris *

Biofilms formed by or entrapping foodborne pathogens pose a significant threat to food safety, as they confer increased resistance to sanitizers and contribute to persistent contamination. Quorum sensing (QS) is a bacterial communication mechanism regulating group behaviors based on population density. In particular, the autoinducer-2 (AI-2) QS enables intra- and interspecies interactions critical for biofilm development in various pathogens. Lactic acid bacteria (LAB), used in food fermentation for centuries, might disrupt QS in pathogens, offering an eco-friendly antibiofilm approach. This study assesses LAB-derived cell-free supernatants (CFSs) to interfere with AI-2-mediated QS and inhibit biofilm formation in *Listeria monocytogenes* and *Staphylococcus aureus*. Neutralized, sterile CFSs from 89 LAB isolates were initially screened for AI-2 QS interference via *Vibrio harveyi* luminescence assays. Twenty active CFSs were further tested at a sub-minimum inhibitory concentration (sub-MIC) for anti-biofilm effects using the conventional microtiter plate assay. The planktonic growth kinetics of the two pathogens exposed to these CFSs were also analyzed in parallel. Results showed that 61.8% of CFSs exhibited AI-2-like signals, while 28.1% significantly inhibited AI-2 QS. Most CFSs with interference reduced *L. monocytogenes* biofilm biomass, and one also decreased *S. aureus* by 45.4%. A specific antibiofilm action not accompanied by any reduction in the planktonic growth rate was evident in most cases. These findings suggest that LAB-derived metabolites target biofilm-specific mechanisms, with data indicating QS interference as a likely contributing factor, although direct evidence in the pathogens remains to be confirmed. Importantly, this approach does not impose selective pressure that might foster antimicrobial resistance. As natural, food-grade organisms, LAB might thus represent a sustainable alternative to synthetic biocides, aligning with environmentally responsible food safety strategies.

Received 14th July 2025
Accepted 23rd October 2025

DOI: 10.1039/d5fb00384a

rsc.li/susfoodtech

Sustainability spotlight

Biofilms of foodborne pathogens, such as *L. monocytogenes* and *S. aureus*, persist in processing environments, compromising food safety and increasing the need for the use of chemical sanitizers. This study introduces a sustainable biocontrol method utilizing cell-free supernatants from lactic acid bacteria (LAB) to disrupt bacterial quorum sensing and biofilm formation, without promoting resistance. These natural, food-grade by-products provide an eco-friendly alternative to synthetic biocides, supporting safer and cleaner food production. This work supports several United Nations Sustainable Development Goals and helps build a more resilient, sustainable food system by reducing reliance on harmful chemicals and promoting microbial ecology-based sanitation strategies.

1. Introduction

Food safety remains a vital concern in the food industry.¹ To secure this, preventing foodborne pathogens from contaminating food and causing illness is essential. Pathogenic bacteria like *Listeria monocytogenes* and *Staphylococcus aureus* thrive in unclean environments; they can adapt and quickly multiply in foods under improper processing and storage, posing serious

health risks to consumers.² According to the latest epidemiological data, listeriosis ranked as the fifth most reported zoonosis in humans in the European Union (EU) in 2023.³ However, it is probably the most serious foodborne disease monitored in the last years by the EU and many other countries around the world, considering the high rates of hospitalization (over 90%) and the increased morbidity and mortality, particularly among the elderly and immunocompromised individuals.⁴ Moreover, *L. monocytogenes* infection during pregnancy, though often mild in the mother, can lead to severe outcomes such as miscarriage, stillbirth, preterm labor, or neonatal sepsis and meningitis, underscoring its significance for food safety

Laboratory of Food Microbiology and Hygiene, Department of Food Science and Nutrition, School of the Environment, University of the Aegean, 81400 Myrina, Lemnos, Greece. E-mail: stagiouris@aegean.gr



and maternal health.⁵ On the other hand, that year, *S. aureus* enterotoxins led to the highest number of hospitalizations within the EU among cases related to foodborne outbreaks caused by bacterial toxins. Both pathogens create strong and persistent biofilms on various food-related and other surfaces.^{6–8}

The biofilms comprising those and other foodborne pathogens and/or spoilage microorganisms are believed to contribute significantly to microbial persistence in the food chain.⁹ These microbial communities attach to surfaces or are associated with interfaces and are embedded in a self-produced (or even acquired) hydrated extracellular matrix.¹⁰ Biofilms represent the primary lifestyle for most microorganisms in natural and man-made environments. These enhance microbial resistance to standard cleaning and disinfection methods and thus enable pathogens to survive and prosper in food production and processing environments, increasing the risk of food contamination and subsequent outbreaks.^{11,12} In recent decades, pathogen biofilm formation in the food industry has garnered attention, making its mitigation an urgent priority for improving food safety and protecting public health.¹³

A key factor in biofilm formation is quorum sensing (QS), a cell-to-cell communication mechanism bacteria use to regulate collective behaviors based on population density.¹⁴ Among the various QS systems, the autoinducer-2 (AI-2) system is particularly notable because it is utilized by a wide range of bacterial species, facilitating both intra- and inter-species communication.¹⁵ Initially discovered in the *Vibrio harveyi* bioluminescence system, the AI-2 QS system allows bacteria to respond to their own AI-2 molecules, as well as those produced by other species. AI-2 signaling and QS, in general, are crucial to bacteria, among others, for coordinating biofilm formation, expressing virulence factors in pathogens, resisting antimicrobials, and adapting to stress.¹⁶ This makes them key targets for interventions aimed at controlling pathogenicity and unwanted bacterial persistence, such as that often encountered in food-related environments.¹⁷ It is also recognized that the conditions within biofilms promote essential cell-to-cell interactions, creating dense, structured populations with advanced organization and communication, like higher multicellular organisms.¹⁸ As biofilms have high cell concentrations, AI activity and QS regulation of gene expression are thus crucial for biofilm physiology.^{19,20} Therefore, disrupting QS could limit unwanted biofilm formation by disturbing bacterial communication.^{21,22}

In both *L. monocytogenes* and *S. aureus*, the AI-2 signaling system has been implicated in modulating biofilm formation and virulence. In *L. monocytogenes*, alterations in AI-2 production have been associated with changes in biofilm structure and density,^{23,24} whereas in *S. aureus*, AI-2 participates in the regulation of genes linked to polysaccharide intercellular adhesin synthesis and surface attachment.^{25,26} Although the precise role of AI-2 in these Gram-positive bacteria appears to be context-dependent, accumulating evidence supports its involvement in biofilm regulation, making it a relevant target for QS interference strategies.

Lactic acid bacteria (LAB) have been used for centuries in food fermentation, enhancing sensory and nutritional profiles

while safeguarding against spoilage and pathogenic organisms.²⁷ Most are safe for consumers, with some also exhibiting probiotic properties that promote human health.²⁸ Interestingly, AI-2 is also recognized for regulating the probiotic activities of LAB.²⁹ These bacteria can produce a variety of bioactive compounds, including organic acids (e.g., lactic, acetic), hydrogen peroxide (H₂O₂), diacetyl, carbon dioxide (CO₂), bacteriocins and other peptides, and have attracted much attention for their potential as natural antimicrobial and anti-biofilm agents.³⁰ Interestingly, some metabolites secreted by LAB have recently been identified as quorum-sensing inhibitors (QSIs), disrupting QS and pathogen communication.^{31–37} Additionally, several LAB strains produce AI-2 signals, enhancing their competitiveness and influencing biofilms and pathogenesis of other harmful bacteria.^{38–41}

The capacity of LAB-derived metabolites to modulate the QS systems of other bacteria may present a promising, eco-friendly strategy for controlling foodborne pathogens and undesired biofilms without relying on traditional chemical sanitizers, which can contribute to antimicrobial resistance and toxic by-products.^{42,43} Interestingly, utilizing these metabolites at sub-inhibitory concentrations for the planktonic growth of target bacteria may lessen selective pressure on them, thus minimizing resistance development.⁴⁴ This is essential due to the increasing resistance of bacterial pathogens to common antibiotics and biocides.⁴⁵

This study investigates the capacity of LAB-derived cell-free supernatants (CFSs) to interfere with AI-2-mediated QS and inhibit biofilm formation in monocultures of *L. monocytogenes* and *S. aureus*. While previous studies have indicated that LAB metabolites can modulate bacterial communication, the link between AI-2-QS interference and biofilm inhibition in key foodborne pathogens remains insufficiently explored. To address this gap, we systematically screened 89 foodborne LAB isolates for AI-2-related activity and evaluated the antibiofilm potential of selected CFSs under sub-minimum inhibitory concentration (sub-MIC) conditions. By connecting QS modulation with targeted biofilm suppression, this work aims to advance our understanding of LAB-derived metabolites as sustainable, low-risk anti-biofilm tools for enhancing food safety. Additionally, its findings provide a foundation for future investigations into the efficacy of LAB-derived AI-2-QS-interfering metabolites against multi-species biofilms under real-world food processing conditions.

2. Materials and methods

2.1. Bacterial strains and culture conditions

All the bacteria used in this study were long-term maintained at –80 °C in cryovials containing porous beads suspended in a cryoprotective fluid (Cryostat; Deltalab, S. L., Rubi, Barcelona, Spain) at the microorganism collection of the Laboratory of Food Microbiology and Hygiene (LFMH) at the University of the Aegean. For the LAB isolates, 89 were chosen from a bigger collection of over 200 foodborne isolates to represent a range of (Repetitive Element Palindromic-PCR; REP-PCR) genotypic patterns, as shown in other parallel experiments (unpublished



results). Of these, 37.1% (33/89) were initially isolated from two types of Greek artisanal (unpasteurized) sheep and goat cheeses (Kalathaki and Melichloro),⁴⁶ while the remaining 62.9% (56/89) were raw sheep milk isolates. The complete list of the tested LAB isolates is provided in Table S1.

To revive the LAB isolates, one cryobead of each one was transferred into 5 mL of De Man, Rogosa, and Sharpe (MRS) broth (Condalab, Madrid, Spain), followed by incubation at 30 °C for 24 to 48 h (until sufficient turbidity of the broth was easily observed, first preculture). Then, 50 µL of each first preculture were transferred to 5 mL of $\frac{1}{4}$ diluted (quarter-strength) Brain Heart Infusion (BHI) broth (Lab M, Heywood, Lancashire, UK) and incubated at 30 °C for 24 h (secondary preculture). Finally, 100 µL of each secondary preculture were transferred to 10 mL of quarter-strength BHI broth and incubated at 30 °C for 20 h under shaking (160 rpm) (working culture). The purity of each LAB working culture was verified by streaking on MRS agar (Condalab) plates. The conditions used to prepare the LAB working cultures (*i.e.*, in quarter-strength BHI broth at 30 °C for 20 h) were based on preliminary experiments that tested various growth media, incubation times, and temperatures to maximize the *V. harveyi* reporter's bioluminescence signal and distinguish between the different isolates' responses (data not presented).

V. harveyi BAA-1117 (BB170) and BAA-1119 (BB152) strains were used for bioluminescence assays. Both strains are mutants derived from the wild-type *V. harveyi* BB120 strain. The *V. harveyi* BAA-1117 (luxN::Tn5 sensor 1⁻ sensor 2⁺) biosensor strain specifically senses the AI-2 molecule, exhibiting luminescence, while *V. harveyi* BAA-1119 (luxL::Tn5 AI-1⁻ AI-2⁺) strain produces only AI-2.⁴⁷ Both *V. harveyi* strains (BAA-1117 and BAA-1119) were originally constructed and characterized by the Bassler Laboratory at Princeton University, as described by Bassler *et al.* (1997).⁴⁷ Before use, each mutant strain was revitalized by transferring one cryobead into 10 mL of Autoinducer Bioassay (AB) medium and incubating at 30 °C for 24 h under shaking (160 rpm) (precultures). AB medium was prepared as previously described.⁴⁸ Then, 100 µL of each preculture were transferred to 10 mL of fresh AB medium and incubated at 30 °C for 16 h under shaking (160 rpm) (working culture). The purity of each *V. harveyi* working culture was verified by streaking on LB agar (Biolab, Budapest, Hungary) plates.

The biofilm-forming assays used the foodborne pathogenic strains *L. monocytogenes* AAL 20107 and *S. aureus* DFSN_B37. The *L. monocytogenes* strain belongs to serovar 1/2 b and was initially isolated from a mixed green salad. The *S. aureus* strain is a cheese isolate. To revitalize the strains, a cryobead for each one was transferred into 5 mL of Tryptic Soy Broth (TSB; Oxoid Limited, Thermo Fisher Scientific Inc., Waltham, MA, USA) and incubated at 37 °C for 24 h (precultures). One hundred µL of each preculture were subsequently transferred into 10 mL of fresh TSB and incubated at 37 °C for 18 h (working cultures). The purity of each working culture was verified by streaking on Tryptic Glucose Yeast Agar (TGYA; Biolife Italiana S. r.l., Milano, Italy) plates.

2.2. Preparation of neutralized and sterile LAB CFSs

Each LAB working culture ($\times 89$) was centrifuged at 4000g for 10 minutes at 4 °C using the Frontier FC5718R Multi Pro tabletop

refrigerated centrifuge (OHAUS Europe GmbH, Nänikon, Switzerland), and the CFS from each was collected and transferred to a new, sterile Falcon® tube, where its pH was adjusted to 6.5 (using 0.5 N NaOH). The neutralized CFSs were then filtered through 0.22 µm syringe filters (Labbox Labware S.L., Barcelona, Spain), and the filtrates were transferred to sterile plastic tubes and stored at -80 °C until further use.

2.3. Screening the LAB CFSs for AI-2-like signal content

The 89 neutralized and sterile LAB CFSs were screened for their potential content of AI-2-like signaling molecules using a previously described bioluminescence method.⁴⁹ First, ten µL of each LAB CFS were added in triplicate to each well of a 96-well polystyrene (PS) microtiter plate (cell culture plate, white, 85.4 × 127.6 mm, flat bottom, SPL Life Sciences, Gyeonggi-do, Korea). A 1 : 5000 dilution of the *V. harveyi* BAA-1117 (BB170) working culture was prepared in AB medium, and 90 µL of that diluted suspension were inoculated into each well. Cell-free supernatant (CFS) from *V. harveyi* BAA-1119 (BB152) strain was used as the positive control (PC) for AI-2 production. This was prepared in AB medium using the procedure previously described to prepare LAB CFSs. Quarter-strength BHI broth and AB medium were used as the medium and negative controls, respectively, instead of LAB CFSs. The microtiter plate was incubated at 30 °C in a Synergy HTX microplate reader (BioTek Instruments Inc., Winooski, Vermont, USA), and bioluminescence was measured every 15 minutes until it increased in the negative control (this increase occurred after approximately 4.5–6 hours). The collected bioluminescence data for each LAB CFC sample were normalized against the medium control ($\frac{1}{4}$ BHI broth), while those from the PC were normalized against the negative control (AB medium) to calculate the Relative Light Units (RLU). These normalizations were carried out by dividing the raw luminescence values recorded for each sample by the corresponding control value at the same point. The representative RLU value for each LAB CFC sample, as well as the PC, was finally determined at the time point when the maximum RLU was observed, which corresponds to the peak of the RLU curve (as a function of incubation time).

2.4. Screening the LAB CFSs for AI-2-QSI

In addition to the AI-2 production bioassay, we aimed to identify any potential inhibition of luminescence production by the biosensor *V. harveyi* BAA-1117 strain because of the LAB CFSs. To do this, an equal volume (five µL) of each neutralized and sterile LAB CFS and the CFS from the AI-2 producer *V. harveyi* BAA-1119 strain was mixed, and the AI-2 activity bioassay was conducted again, as previously outlined. In this assay however, only the CFSs that did not induce luminescence production in the *V. harveyi* BAA-1117 strain ($n = 34$) were tested, as indicated by the results of the experiment described in the previous section. The CFS from the *V. harveyi* BAA-1119 strain served as a PC (indicating no AI-2 inhibition), using five µL of that CFS and five µL of AB medium for this purpose. The inhibition of AI-2 QS activity was reported as the percentage of luminescence (RLU) of each LAB CFS sample relative to that of the corresponding PC: $100 - [(RLU_{\text{sample}}/RLU_{\text{PC}}) \times 100]$.⁴⁸



2.5. Preparation of saline suspension for each pathogen (*L. monocytogenes* and *S. aureus*)

Each pathogen's 10 mL working culture (10^{8-9} CFU mL⁻¹) was centrifuged at 4000g for 10 minutes at 4 °C. The supernatant was discarded, and the bacterial pellet was suspended in 10 mL of quarter-strength Ringer's solution (Lab M). A second centrifugation was conducted under the same conditions as the first to wash the cells. The new bacterial pellet was resuspended in 10 mL of quarter-strength Ringer's solution, and its absorbance at 600 nm ($A_{600\text{ nm}}$) was then adjusted to 0.1 using a tabletop visible spectrophotometer (VIS-7220 G, Beijing Rayleigh Analytical Instrument Corporation, Beijing, China). The cellular concentration of each saline suspension was determined through plate counting on TGYA and was found to be approximately 10^8 CFU mL⁻¹.

2.6. Selection of AI-2-QS-interfering LAB CFCs and determination of their MICs against each pathogen

Twenty LAB CFSs that were found to modulate *V. harveyi* AI-2-QS induced bioluminescence significantly (containing either AI-2-like signals or presenting AI-2 QSI) were selected to represent a variety of LAB species. The MIC of each one was then determined against the planktonic growth of each of the two pathogens (*L. monocytogenes* and *S. aureus*) using the classical broth microdilution method, as previously described.⁵⁰ In summary, ten different concentrations of each neutralized and sterile LAB CFS ranging from 50% to 0.1% v/v were prepared *via* two-fold dilutions in TSB. The first of those dilutions (50% v/v) was made by mixing equal volumes of each CFS (100% v/v) with double-strength TSB (dsTSB) to make up for the dilution of nutrients. The dsTSB was prepared according to the manufacturer's instructions but with double the usual amount of powder. One hundred and ninety-eight (198) µL of each of those dilutions ($\times 10$) were then added in duplicate to the wells of a sterile 96-well PS microtiter plate (transparent, flat, Cat. No. 30096, SPL Life Sciences) and inoculated with 2 µL of each saline bacterial suspension ($A_{600\text{ nm}} = 0.1$) that was previously diluted 1:10 to achieve an initial concentration of approximately 10^5 CFU mL⁻¹ for each pathogen. In the PC, quarter-strength BHI broth was utilized instead of CFS, while the negative control (NC) consisted of equal volumes (100 µL each) of sterile dsTSB and quarter-strength BHI broth (with no LAB CFS added and no bacterial inoculation). The plate was covered with parafilm and incubated at 37 °C for 24 h. Growth in each well was ultimately assessed turbidimetrically through visual observation. For each pathogen, the MIC of each LAB CFS was determined as its lowest concentration inhibiting the visible bacterial growth.

2.7. Planktonic growth of each pathogen in the presence of sub-MIC of each selected AI-2-QS-interfering LAB CFS and determination of growth kinetic parameters

For each pathogen (*L. monocytogenes* and *S. aureus*), a 1:100 dilution of its saline suspension ($A_{600\text{ nm}} = 0.1$) was prepared in dsTSB, resulting in a cell concentration of approximately 10^6

CFU mL⁻¹. Subsequently, 100 µL of that diluted suspension was transferred into each well ($\times 100$) of the Bioscreen honeycomb plate (Oy Growth Curves Ab Ltd, Turku, Finland), followed by the quadruplicate addition of 100 µL of each neutralized and sterile LAB CFS ($\times 20$). This yielded an initial bacterial cell concentration of 5×10^5 CFU mL⁻¹, with each CFS tested at a 50% v/v concentration (previously verified as a sub-MIC). In the case of PC, quarter-strength BHI broth was used in the place of CFS. Conversely, the NC comprised equal volumes (100 µL each) of sterile dsTSB and quarter-strength BHI broth (with no LAB CFS addition and no bacterial inoculation). The prepared plate was finally incubated at 37 °C for 24 h in the heated chamber of the Bioscreen C° Pro instrument (Oy Growth Curves Ab Ltd), which was set to record the optical density of the contents of each well at 600 nm ($OD_{600\text{ nm}}$) every 30 minutes. Before each measurement, the plate was automatically shaken for 5 seconds.

For each treatment (two pathogens $\times 20$ LAB CFS, including the positive and negative controls), the BioScreener PRO Software automatically generated a growth curve ($OD_{600\text{ nm}}$ vs. time). The data from all the growth curves ($n = 352$) were exported to the Excel® module of Microsoft® Office 365 (Redmond, WA, USA) for further processing (Fig. S1). This processing involved fitting all the OD time curves to the Baranyi and Roberts model⁵¹ to determine detection times (h), maximum slope rates of OD changes (MSrODc; $OD_{600\text{ nm}}\text{ h}^{-1}$), and final $OD_{600\text{ nm}}$ values. This fitting was conducted using the web edition of DMFit, which is freely accessible at ComBase (<https://combasebrowser.errc.ars.usda.gov/>). In the case of *S. aureus*, only the OD data obtained during the first 12 h of incubation were used for fitting, as the stationary phase OD values increased unexpectedly after that time (Fig. S1B). The average (mean) values of kinetic parameters for each treatment and their standard deviations were finally determined.

2.8. Biofilm growth of each pathogen in the presence of sub-MIC of each selected AI-2-QS-interfering LAB CFS

Initially, for each pathogen (*L. monocytogenes* and *S. aureus*), 200 µL of its saline suspension ($A_{600\text{ nm}} = 0.1$) were transferred into each well of a sterile 96-well PS microtiter plate (transparent, flat, Cat. No. 30096, SPL Life Sciences) using a micropipette. The plate was then covered with its lid and incubated at 37 °C for two hours to facilitate bacterial cell adhesion. After the adhesion phase, the bacterial suspension was carefully removed from each well using a multichannel pipette, ensuring that the planktonic cells were entirely discarded. To wash and eliminate any loosely attached cells, 200 µL of quarter-strength Ringer's solution were added to each well and subsequently removed. Following washing, 100 µL of double-strength (ds) of the respective nutrient medium for each pathogen (see below) and 100 µL of each (100% v/v) neutralized and sterile LAB CFS ($\times 20$) were added in duplicate to each well. This resulted in an initial CFS concentration of 50% v/v (previously verified as a sub-MIC). The double concentration of nutrients for the media supporting the biofilm growth of pathogens was used to compensate for the dilution of nutrients from the simultaneous addition of CFS.



Brain Heart Infusion (BHI) broth served as the nutrient medium for the biofilm growth of *L. monocytogenes*, while TSB enriched with additional sodium chloride (NaCl) and glucose was utilized for *S. aureus* (with final NaCl and glucose concentrations of 5% w/v and 1% w/v, respectively). Those optimized biofilm-forming media for each pathogen, resulting in the highest and most stable biofilm biomass after 48 h of incubation, were determined through preliminary experiments (data not presented). The lid was finally placed on the microtiter plate, which was sealed with parafilm to prevent media evaporation, and incubated at 37 °C for 48 h to facilitate biofilm formation. In the PC, quarter-strength BHI broth was used instead of CFS. Conversely, for the NC, sterile quarter-strength Ringer's solution replaced saline bacterial suspension ($A_{600\text{ nm}} = 0.1$) during the initial two-hour adhesion phase, with all other subsequent treatments remaining identical. The selected incubation time (48 h) and temperature (37 °C) correspond to conditions previously validated to yield mature, stable biofilms for both pathogens, ensuring reproducibility. All experiments were performed in duplicate, and each included both positive (untreated) and negative (cell-free) controls. This standardized microtiter plate protocol, based on widely accepted methods for quantifying biofilm formation in foodborne bacteria (and others as well), allows reliable comparison across treatments and minimizes variability due to surface effects or other factors.

2.9. Assessment of pathogen biofilm biomass accumulated on PS in the presence of sub-MIC of each selected AI-2-QS-interfering LAB CFS

After the 48-h biofilm incubation period, the absorbance at 600 nm ($A_{600\text{ nm}}$) of the planktonic cultures found in each well of the PS microtiter plate was measured using a multimode microplate reader (Tecan Spark®, Tecan Group Ltd, Männedorf, Switzerland), indirectly assessing the planktonic growth in each well. The planktonic cultures were then discarded by forcefully inverting the plate over an aluminum pan containing household bleach. To further wash the wells and remove any loosely attached cells, 200 µL of quarter-strength Ringer's solution were added to each well and subsequently removed with a multichannel pipette. This washing was repeated to ensure the complete removal of any remaining loosely attached cells. For biofilm staining, 200 µL of a 0.1% (w/v) crystal violet (CV) solution (1% w/v, aqueous solution; Sigma-Aldrich Chemie GmbH, Taufkirchen, Germany) were added to each well. The microtiter plate was gently agitated by hand, entirely covered with aluminum foil, and left at room temperature for 15 minutes to allow the biofilms to absorb the stain. Following staining, the CV solution was discarded, and the wells were rinsed three times with deionized water to eliminate any excess dye. To solubilize the biofilm-bound CV, 200 µL of an ethanol:acetone solution (80:20, v/v) were then added to each well. The microtiter plate was gently agitated, sealed with its lid, and incubated at 4 °C for 15 minutes (to allow homogenization of the dye solution). Finally, the absorbance at 590 nm ($A_{590\text{ nm}}$) of the solubilized CV was measured using the Tecan Spark® microplate reader, indirectly assessing the pathogen biofilm biomass accumulation in each well.

2.10. Statistics

Each experiment was conducted twice, beginning with independent bacterial cultures. The resulting data on planktonic growth kinetic parameters (detection times, MSrODc, and final OD_{600 nm} values) and biofilm biomasses ($A_{590\text{ nm}}$) underwent one-way analyses of variance (ANOVA), followed by Tukey's Honestly Significant Difference (HSD) post hoc tests for mean pairwise comparisons to identify any significant differences between the different treatments (including both positive and negative controls). Pearson correlation analysis was also used to determine any correlation between biofilm biomasses ($A_{590\text{ nm}}$) and surrounding planktonic absorbances ($A_{600\text{ nm}}$). All analyses were completed utilizing the statistical software STATISTICA® (StatSoft Inc., Tulsa, OK, USA). All differences are reported at a significance level of 0.05.

3. Results and discussion

3.1. Relative AI-2-like activity and AI-2 QSI of the LAB CFSs

Fig. 1 illustrates a pie chart categorizing the 89 foodborne LAB isolates based on the ability of their neutralized and sterile CFSs to induce luminescence production in the *V. harveyi* BAA-1117 reporter strain (sensor 1⁻, sensor 2⁺), suggesting that they secrete metabolites with AI-2-like QS activity. These findings show that 61.8% (55/89) of the CFSs could induce luminescence in the reporter strain with RLU ≥ 10, while the remaining CFSs (38.2%; 34/89) demonstrated only a low level of signal induction (RLU < 10). Notably, 14.6% of the CFSs (13/89) elicited a strong bioluminescence response (RLU > 100), likely indicating their high content of AI-2-like molecules compatible with the receptors of the reporter. The detailed data on the relative AI-2-like activity for each LAB CFS, along with that of PC (*i.e.*, the CFS of the *V. harveyi* BAA-1119 strain), is presented in Table S1.

Table 1 presents the percentage of AI-2-like activity inhibition for each of the 34 LAB CFSs that could not produce strong AI-2-like signals (RLU < 10) when evaluated in the *V. harveyi* BAA-1117 AI-2 induction assay. These findings emphasize the strong AI-2 inhibitory capacity of most of these tested CFSs. Therefore, included among them are the CFSs from 25 isolates (28.1%; 25/89) that demonstrated robust AI-2 QSI activity,

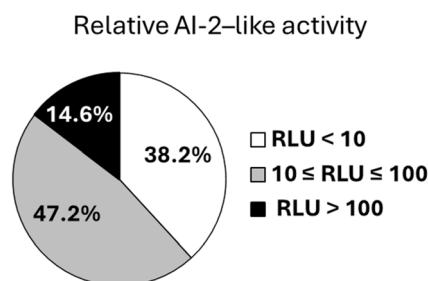


Fig. 1 Pie chart of the categorization of the 89 foodborne LAB isolates according to the ability of their neutralized and sterile CFSs to induce luminescence production by the *V. harveyi* BAA-1117 strain, indicating that they secrete metabolites with AI-2-like QS activity. Luminescence production is expressed as Relative Light Units (RLU) and categorized into <10, ≥10 and ≤100, and >100.



Table 1 Percentage (%) inhibition of AI-2-like activity for each of the 34 LAB CFSs that were incapable of producing strong AI-2-like signals (RLU < 10) when assessed in the *V. harveyi* BAA-1117 AI-2 induction assay. Values represent mean values \pm standard deviations. The 25 isolates whose CFS could inhibit more than 90% of the bioluminescence of the PC (*V. harveyi* BAA-1119) strain are displayed in bold

s/n	Isolate code	LAB species	% Inhibition of AI-2-like activity
1	DFSN_B43	<i>Enterococcus</i> sp	87.48 \pm 4.81
2	DFSN_B44	<i>Lactacaseibacillus paracasei</i>	84.09 \pm 3.40
3	DFSN_B54	<i>Pediococcus pentosaceus</i>	63.37 \pm 14.53
4	LFMH_B2	<i>Lactacaseibacillus</i> sp	92.09 \pm 2.04
5	LFMH_B10	<i>Pediococcus acidilactici</i>	90.94 \pm 8.10
6	LFMH_B17	<i>Enterococcus avium</i>	91.92 \pm 0.70
7	LFMH_B19	<i>Enterococcus durans</i>	90.17 \pm 0.31
8	LFMH_B25	<i>Enterococcus hirae</i>	96.22 \pm 0.68
9	LFMH_B26	<i>Enterococcus faecium</i>	84.14 \pm 0.29
10	LFMH_B29	<i>Lactobacillus delbrueckii</i>	94.45 \pm 1.43
11	LFMH_B34	<i>Enterococcus faecium</i>	89.56 \pm 5.06
12	LFMH_B35	<i>Enterococcus faecium</i>	97.20 \pm 0.60
13	LFMH_B36	<i>Enterococcus faecalis</i>	95.97 \pm 0.29
14	LFMH_B42	<i>Streptococcus macedonicus</i>	96.38 \pm 1.02
15	LFMH_B43	<i>Streptococcus lutetiensis</i>	94.41 \pm 4.39
16	LFMH_B44	<i>Streptococcus lutetiensis</i>	98.27 \pm 0.02
17	LFMH_B45	<i>Streptococcus gallolyticus</i> subsp. <i>macedonicus</i>	98.71 \pm 0.34
18	LFMH_B46	<i>Streptococcus gallolyticus</i> subsp. <i>macedonicus</i>	98.46 \pm 1.11
19	LFMH_B47	<i>Lactobacillus delbrueckii</i>	93.11 \pm 7.23
20	LFMH_B52a	<i>Enterococcus</i> sp	94.59 \pm 1.93
21	LFMH_B54	<i>Limosilactobacillus fermentum</i>	95.25 \pm 0.16
22	LFMH_B57a	<i>Enterococcus</i> sp	94.97 \pm 0.02
23	LFMH_B58	<i>Limosilactobacillus fermentum</i>	91.11 \pm 2.46
24	LFMH_B59	<i>Limosilactobacillus fermentum</i>	93.37 \pm 3.71
25	LFMH_B63a	<i>Lactacaseibacillus</i> sp	90.91 \pm 6.15
26	LFMH_B65a	<i>Limosilactobacillus</i> sp	90.57 \pm 2.09
27	LFMH_B65b	<i>Limosilactobacillus</i> sp	88.97 \pm 4.87
28	LFMH_B66	<i>Lactacaseibacillus rhamnosus</i>	91.78 \pm 1.33
29	LFMH_B69	<i>Lactacaseibacillus rhamnosus</i>	92.09 \pm 3.96
30	LFMH_B72	<i>Lactacaseibacillus rhamnosus</i>	94.89 \pm 4.32
31	LFMH_B75	<i>Lactacaseibacillus rhamnosus</i>	92.08 \pm 1.44
32	LFMH_B76	<i>Lactobacillus delbrueckii</i>	84.93 \pm 2.39
33	LFMH_B78	<i>Limosilactobacillus fermentum</i>	84.71 \pm 5.84
34	LFMH_B79a	<i>Lactacaseibacillus rhamnosus</i>	89.09 \pm 6.41

achieving at least 90% inhibition of the luminescence of the PC (*V. harveyi* BAA-1119 strain). To confirm that the observed reduction in luminescence was not due to growth inhibition of the reporter strain, all 34 LAB CFSs were also tested at 5% (v/v) for their effect on *V. harveyi* BAA-1117 growth using the Bioscreen C° Pro instrument; no significant inhibition was detected (data not shown).

Our results showing that 61.8% (55/89) of the LAB CFSs induced luminescence in the reporter strain are consistent with earlier research, which found that 76.4% of 89 LAB strains from minced beef exhibited AI-2-like activity.⁵² In that study, *Leuconostoc* spp. were predominant in AI-2 production, while *Lactobacillus sakei* (now *Latilactobacillus sakei*) strains did not show detectable activity. Our findings similarly identified AI-2-like activity in our sole *Leuconostoc mesenteroides* isolate, but no *L. sakei* strains were included in our dataset. Comparatively, a study examining 229 LAB isolates from kimchi found species-specific AI-2 activity: *Lactobacillus plantarum* (now *Lactacaseibacillus plantarum*) and *Lactobacillus brevis* produced AI-2, while *L. sakei* and *Lactobacillus curvatus* (now *Latilactobacillus curvatus*)

were associated with AI-2 inhibition.⁵³ Interestingly, some strains like *Weissella cibaria* showed both effects depending on the isolate. Our results similarly revealed intraspecies variability among strains (including *Enterococcus faecium*, *Enterococcus faecalis*, *Limosilactobacillus fermentum*, and *Lactacaseibacillus rhamnosus* species), suggesting that quorum-modulating activity is strain-specific.

3.2. Determination of the MIC and effect of sub-MIC of each selected AI-2-QS-interfering LAB CFS on the planktonic growth of each pathogen

The 20 selected AI-2-QS-interfering LAB CFSs are shown in Table 2. Of these, 16 were found to significantly induce *V. harveyi* luminescence (RLU \geq 10) indicating that they contained AI-2-like signals, while the remaining four inhibited that light induction, indicating that they presented AI-2 QSI. For all those CFSs, their MIC against each pathogen's planktonic growth (*L. monocytogenes* and *S. aureus*) exceeded 50% v/v since the TSB media in all treatment wells of the broth microdilution method appeared turbid after 24 hours of incubation (at 37 °C). To



Table 2 Significant effects ($p < 0.05$) of the presence of each of the 20 selected AI-2-QS-interfering LAB CFSs (applied at 50% v/v) on the growth kinetic parameter values [detection times (h), MSrODc ($\text{OD}_{600 \text{ nm}} \text{ h}^{-1}$), and final $\text{OD}_{600 \text{ nm}}$ values] for the two pathogens (*L. monocytogenes* and *S. aureus*) during their planktonic growth (in TSB at 37 °C for 24 h) compared to each respective PC (without LAB CFS addition). The dashes (—) signify no substantial influence ($p > 0.05$)

s/n	Isolate code	LAB species	AI-2 QS interference	<i>L. monocytogenes</i>			<i>S. aureus</i>		
				Detection time (h)	MSrODc ($\text{OD}_{600 \text{ nm}} \text{ h}^{-1}$)	Final $\text{OD}_{600 \text{ nm}}$ value	Detection time (h)	MSrODc ($\text{OD}_{600 \text{ nm}} \text{ h}^{-1}$)	Final $\text{OD}_{600 \text{ nm}}$ value
1	LFMH_B7	<i>Enterococcus pseudoavium</i>	Induction	—	Decrease	—	Increase	—	—
2	LFMH_B18	<i>Lactococcus lactis</i> subsp. <i>lactis</i>	Induction	Increase	Decrease	—	Increase	—	—
3	LFMH_B23	<i>Lactococcus garviae</i>	Induction	—	—	—	Increase	—	—
4	LFMH_B31	<i>Enterococcus faecium</i>	Induction	—	—	—	—	—	—
5	LFMH_B51	<i>Enterococcus durans</i>	Induction	—	—	—	—	—	—
6	LFMH_B53	<i>Limosilactobacillus fermentum</i>	Induction	—	—	—	—	—	—
7	LFMH_B63b	<i>Enterococcus</i> sp	Induction	—	—	—	—	—	—
8	LFMH_B68	<i>Enterococcus faecalis</i>	Induction	—	—	—	—	—	—
9	LFMH_B70	<i>Lacticaseibacillus rhamnosus</i>	Induction	—	—	—	—	—	—
10	LFMH_B79b	<i>Enterococcus faecium</i>	Induction	Increase	Decrease	—	—	—	—
11	LFMH_B81	<i>Enterococcus pseudoavium</i>	Induction	—	—	—	—	—	—
12	LFMH_B82	<i>Leuconostoc mesenteroides</i>	Induction	—	—	—	—	Decrease	—
13	LFMH_B83	<i>Lactococcus lactis</i>	Induction	—	Decrease	—	—	Decrease	—
14	DFSN_B50	<i>Enterococcus glivus</i>	Induction	—	—	—	—	Decrease	—
15	DFSN_B55	<i>Enterococcus</i> sp	Induction	Increase	Decrease	Decrease	—	Decrease	—
16	DFSN_B58	<i>Pediococcus pentosaceus</i>	Induction	Increase	Decrease	Decrease	Increase	Decrease	—
17	LFMH_B10	<i>Pediococcus acidilactici</i>	Inhibition	—	—	—	—	—	—
18	LFMH_B44	<i>Streptococcus lutetiensis</i>	Inhibition	—	—	—	—	—	—
19	LFMH_B45	<i>Streptococcus gallolyticus</i> subsp. <i>macedonicus</i>	Inhibition	—	—	—	—	Decrease	—
20	LFMH_B69	<i>Lacticaseibacillus rhamnosus</i>	Inhibition	—	—	—	—	—	—

quantify pathogen's planktonic growth in more detail, three kinetic parameters were derived from the fitted $\text{OD}_{600 \text{ nm}}$ curves using the Baranyi and Roberts model: detection time (h; reflecting the lag phase), MSrODc ($\text{OD}_{600 \text{ nm}} \text{ h}$; growth rate), and final $\text{OD}_{600 \text{ nm}}$ (plateau cell density).⁵¹ These parameters, as validated in earlier works, reliably indicate changes in planktonic growth behavior.^{54–56} The significant effects ($p < 0.05$) of the presence of each of the 20 selected AI-2-QS-interfering LAB CFSs (each applied at 50% v/v) on the values of these growth kinetic parameters for the two pathogens (*L. monocytogenes* and *S. aureus*) during their planktonic growth (in TSB at 37 °C for 24 h) compared to each respective PC (without LAB CFS addition) are presented in Table 2. The average kinetic parameters for each pathogen and treatment, used to determine those effects, are displayed in Fig. S2. The original average OD time curves are provided in Fig. S1. It can be concluded that most of the LAB CFSs tested did not significantly affect the planktonic growth of the two pathogens. However, there were some CFSs (e.g., CFS from the DFN-B58 LAB isolate; s/n 16) that significantly delayed pathogen growth ($p < 0.05$), as demonstrated by the increased detection time and the accompanying decrease in the MSrODc, indicating a negative impact on the planktonic growth rates of both pathogens. As another example, the CFS from the DFN-B79b LAB isolate (s/n 10) significantly ($p < 0.05$) delayed the growth of the *L. monocytogenes* strain without causing any significant effect on the growth of the *S. aureus* strain. It should,

however, be noted that in all treatments (except for NCs), the planktonic growth of the two pathogens led to sufficient turbidity in the well contents at the end of the 24-hour incubation. Visual inspection also confirmed this, indicating that all LAB CFSs ($\times 20$) were applied at a sub-MIC (50% v/v).

3.3. Effect of sub-MIC of each selected AI-2-QS-interfering LAB CFS on the biofilm growth of each pathogen

The biofilm assays were conducted under standardized and optimized conditions to ensure reproducibility, with all parameters -including incubation time, temperature, surface type, and medium composition-carefully controlled to promote consistent biofilm development in both pathogens. The biofilm biomasses ($A_{590 \text{ nm}}$) of each pathogen (*L. monocytogenes* and *S. aureus*) accumulated on the surface of the 96-well PS microtiter plates following the static incubation at 37 °C for 48 h in the presence of each of the 20 selected AI-2-QS-interfering LAB CFSs (each applied at 50% v/v) are shown in Fig. 2. The absorbances of the planktonic suspensions ($A_{600 \text{ nm}}$) found in each well at the sampling time (48 h) are also indicated for each treatment in the same figure. It can be concluded that nearly all CFSs, except for two (derived from the LAB isolates LFMH_B7 and LFMH_B31), significantly inhibited biofilm formation by *L. monocytogenes* (30.4–58.0% reduction in biofilm biomass). The highest inhibition occurred when the pathogen was allowed to form biofilm in the presence of fermentation-derived



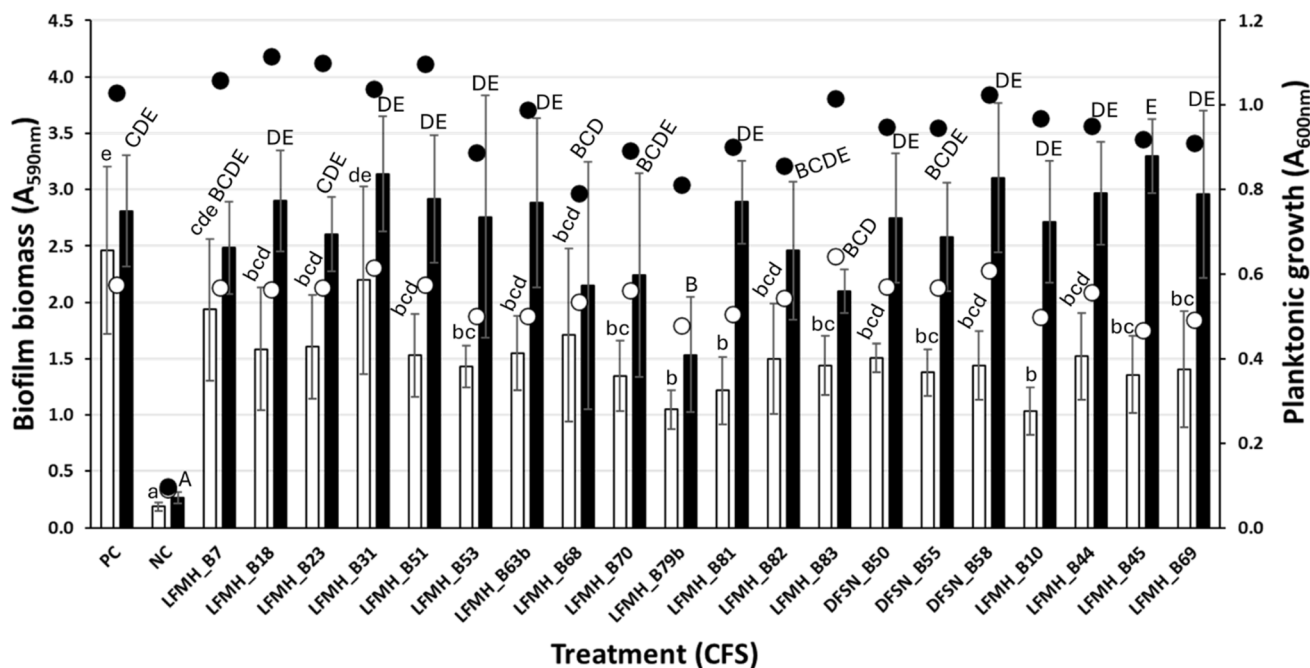


Fig. 2 Biofilm biomasses ($A_{590\text{ nm}}$) of the two pathogens (*L. monocytogenes* □ and *S. aureus* ■) accumulated on the surface of the 96-well PS microtiter plate after incubation at 37 °C for 48 h in the presence of each of the 20 selected AI-2-QS-interfering LAB CFSs (each applied at 50% v/v). The bars indicate the mean values \pm standard deviations. The accumulated biofilm biomasses for PC and NC are also displayed (on the right). The absorbances of the planktonic suspensions ($A_{600\text{ nm}}$) found in each well at the sampling time (48 h) are also presented for each treatment (as white ○ and black ● circles for *L. monocytogenes* and *S. aureus*, respectively). The planktonic means' standard deviation bars have been omitted to enhance clarity. For each pathogen individually, biofilm biomass mean values followed by different superscript letters are significantly different ($p < 0.05$).

metabolites produced by the LAB isolates LFMH_B79b and LFMH_B10 (corresponding to *Enterococcus faecium* and *Pediococcus acidilactici*, respectively). In these cases, the accumulated biofilm biomass was reduced by 57.3% and 58.0%, respectively, compared to the PC. Regarding *S. aureus*, only the CFS from the *E. faecium* LFMH_B79b isolate significantly reduced the pathogen's biofilm formation, showing a 45.4% reduction in biomass compared to the PC. A linear correlation between the number of planktonic cells found in each well at the sampling time (48 h) and the biofilm biomass surrounding that well is also evident when considering the absorbance values exhibited together by both pathogens (Fig. 3). Thus, the higher concentrations of planktonic cells observed for *S. aureus* coincide with its greater biofilm-forming ability compared to *L. monocytogenes*.

It should be highlighted that none of the selected CFSs inhibited visible growth of *L. monocytogenes* or *S. aureus* at this concentration (50% v/v), and planktonic growth kinetics analysis revealed no substantial impact on lag time, growth rate, or final OD values for most treatments. This observation supports the hypothesis that the CFSs' antibiofilm effects are not due to growth suppression but rather reflect a biofilm-specific mechanism—possibly through interference with QS, inhibition of attachment, or disruption of aggregation. Similar observations have been reported in other studies by both our team and others, where subinhibitory concentrations of lactic acid and other bioactive compounds, such as thymol, disrupted biofilm

formation by foodborne pathogens through non-lethal mechanisms when applied at sub-MIC values.^{57,58} In addition, this biofilm inhibition that was observed here did not correlate with whether the CFS contained AI-2-like signals or showed QS-inhibitory activity. For instance, both *E. faecium* LFMH_B79b (AI-2 producer) and *Pediococcus acidilactici* LFMH_B10 (QS inhibitor) yielded the most substantial antibiofilm effects. This suggests that different mechanisms—either AI-2 mimicry or interference—may achieve similar antibiofilm outcomes. Nonetheless, these findings do not exclude the possibility that other regulatory or physicochemical factors unrelated to AI-2 signaling also contribute to the observed antibiofilm effects. In addition, only *E. faecium* LFMH_B79b significantly reduced biofilm in both pathogens, highlighting potential species-specific or strain-specific effects.

Our findings also align with previous work indicating that LAB-derived compounds can inhibit biofilm formation through QS interference. For example, a previous study demonstrated that *L. sakei* inhibited AI-2 signaling and virulence traits in enterohaemorrhagic *Escherichia coli* O157:H7, reducing motility, attachment, biofilm biomass, and virulence gene expression—without affecting viability.⁵⁹ It should be noted, however, that the QS circuitry of *E. coli*—which appears to primarily rely on AI-2 signaling—differs substantially from that of *S. aureus* and *L. monocytogenes*, both of which possess additional, species-specific systems such as the agr network;²⁶ thus, the effects observed in Gram-negative models cannot be directly



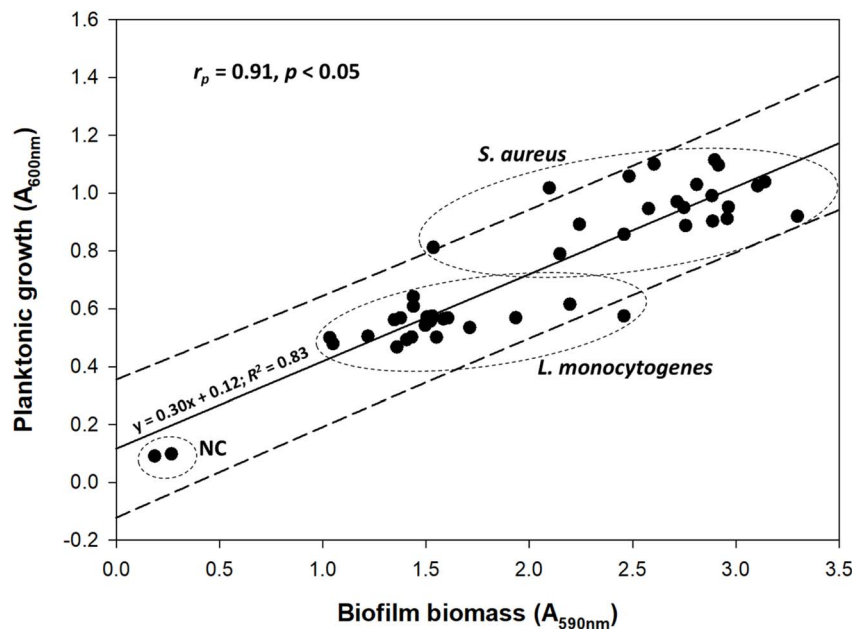


Fig. 3 Correlation between biofilm biomasses ($A_{590\text{ nm}}$) on the surface of the 96-well PS microtiter plate and surrounding planktonic absorbances ($A_{600\text{ nm}}$) after 48 h of incubation at 37 °C. The solid line represents the linear regression equation, while the dotted lines indicate the prediction intervals ($\alpha = 0.95$). Pearson's correlation coefficient (r_p), p -value, the mathematical equation of the linear regression plot, and its regression coefficient (R^2) are also presented. Dots denote the mean values of all experiments ($n = 44$, two pathogens \times 22 treatments, as shown in Fig. 2). The standard deviation bars have been omitted for clarity. NC represents negative controls (absence of bacterial presence).

extrapolated to these Gram-positive pathogens. Similarly, another study found that *Weissella viridescens* and *Weissella confusa* reduced AI-2 activity and biofilm formation by *Salmonella enterica* serovars Typhi and Typhimurium.³⁴ Other studies also highlight concurrent anti-QS, anti-biofilm, and anti-virulence effects by LAB metabolites.^{60–63} Despite these promising results, our data indicate that LAB antibiofilm activity is more pronounced against *L. monocytogenes* than *S. aureus*. Similar assays using *Pseudomonas aeruginosa*, a robust Gram-negative biofilm former, did not yield significant results (data not shown), emphasizing potential limitations and target specificity. This variation likely reflects fundamental differences in the biofilm and QS regulatory networks among different bacteria, which may modulate or override AI-2-related responses.

Microbial biofilms pose a significant challenge in the food industry due to their enhanced tolerance to environmental stressors and resistance to sanitation methods.⁹ The AI-2 QS system, a widely conserved signaling mechanism that facilitates interspecies and intraspecies bacterial communication, plays a crucial role in regulating virulence and biofilm formation.¹⁶ Notably, some LAB produce metabolites capable of modulating AI-2 QS, thereby inhibiting pathogenic bacteria by competing their biofilm formation.^{38–41,64} These QS-interfering mechanisms are particularly promising, as they may inhibit biofilm development without imposing intense selective pressure, thereby minimizing the risk of resistance development.⁴⁴ Building on these findings, our study evaluated the potential of CFSs from various foodborne LAB species to disrupt AI-2 QS and inhibit biofilm formation by two significant foodborne

pathogens: *L. monocytogenes* and *S. aureus*. Both pathogens are known to use AI-2 for QS and possess additional systems, such as the Agr QS system, which employs autoinducing peptides (AIPs) to regulate biofilm development and virulence.^{23–26,65–67}

In *L. monocytogenes*, the role of AI-2 in biofilm formation is complex. Early studies showed that *luxS* mutants, deficient in AI-2 synthesis, formed denser biofilms than the wild-type, and synthetic AI-2 could not restore the original phenotype.^{23,24} However, more recent reports demonstrate that AI-2 disruption using natural compounds, such as bacteriocins, can significantly reduce biofilm formation in *L. monocytogenes*.^{68–70} Similarly, in *S. aureus*, AI-2 appears to repress biofilm development by downregulating the *rbf* gene, which positively influences *ica* operon expression responsible for polysaccharide intercellular adhesin (PIA) synthesis.²⁵ Additional studies have shown that AI-2 promotes *icaR* expression, thereby further inhibiting PIA synthesis and biofilm formation.⁶⁷ Notably, in contrast to *L. monocytogenes*, the addition of synthetic AI-2 restored biofilm formation in *S. aureus luxS* mutants, confirming its signaling role.²⁵ Surfactin, a biosurfactant produced by *Bacillus subtilis*, has also been shown to elevate AI-2 levels and suppress *S. aureus* biofilms.⁷¹ Nonetheless, not all studies agree; some found that *luxS* inactivation had no discernible effect on virulence or biofilm traits.⁷² Still, many compounds, including LAB-derived biosurfactants, have been shown to inhibit *S. aureus* biofilms by disrupting AI-2 QS.^{73–78} These mixed findings suggest that AI-2's role in Gram-positive bacterial biofilm formation, particularly in *L. monocytogenes* and *S. aureus*, is nuanced and context-dependent.



Although our study offers additional insight into this critical aspect, the presence of AI-2-related activity in a CFS does not necessarily explain its antibiofilm effect. Undoubtedly, other bioactive molecules in the CFS—such as biosurfactants, exopolysaccharides, enzymes, oxidative agents, and peptides—may act independently or synergistically with QS interference. Therefore, beyond QS modulation, other mechanisms may also underlie the antibiofilm effects observed. For instance, LAB secreted metabolites can alter surface properties, impede initial bacterial adhesion, or destabilize the extracellular matrix.³⁰ Such activities could weaken biofilm integrity or prevent its establishment even in the absence of direct QS interference. Given that the present CFSs were neutralized and tested at sub-MIC levels, these alternative or complementary actions likely act in concert with any possible QS modulation rather than through simple antimicrobial pressure. Future studies should aim to identify the specific bioactive metabolites and characterize the LAB strains responsible for these effects through targeted chemical and molecular analyses. Such work will clarify the mechanisms underlying LAB-mediated biofilm inhibition and support the development of defined, strain-specific biocontrol formulations.

It should also be noted that although the *V. harveyi* bioluminescence assays provided clear evidence that many LAB-derived CFSs could modulate AI-2 activity—either by mimicking or inhibiting the signal—this method only reflects potential interactions with the conserved AI-2 signaling pathway and cannot directly demonstrate that the observed biofilm inhibition in *L. monocytogenes* and *S. aureus* is caused by disruption of their respective AI-2 systems. As already mentioned, these pathogens also possess additional, species-specific QS circuits (e.g., the Agr system), which may interact with or override AI-2 signaling. Therefore, while the patterns observed are consistent with a QS-mediated mechanism, confirmation will require direct molecular evidence. Future studies should assess whether exposure to active LAB CFSs alters the expression of QS-related genes (e.g., *luxS*, *agrA*, *agrC*), modifies AI-2 levels during biofilm development, or yields comparable antibiofilm effects in QS-deficient mutants. Incorporating such analyses would help establish a mechanistic link between AI-2 modulation and biofilm suppression by LAB metabolites, providing greater specificity and depth to the proposed model.

4. Conclusions and future perspectives

In conclusion, this study demonstrates that food-derived LAB can produce extracellular metabolites that interfere with AI-2 QS and inhibit biofilm formation in *L. monocytogenes* and, to a lesser extent, *S. aureus*. These findings support the potential use of LAB metabolites as sustainable, food-safe antibiofilm agents. The current data suggest that QS interference is a likely mechanism underlying the observed antibiofilm effects; however, direct confirmation within the pathogens' own QS networks remains to be established through targeted molecular

analyses. Future research should therefore investigate whether these metabolites alter QS gene expression, signaling molecule dynamics, or biofilm-associated phenotypes in QS-deficient mutants. The chemical identification of these metabolites is also crucial. To enhance industrial applicability, further work should evaluate the stability, safety, and efficacy of these metabolites under realistic conditions involving multi-species biofilms in food processing. Additionally, exploring synergistic approaches that combine LAB-derived compounds with other natural biofilm disruptors, such as bacteriocins, organic acids, or enzymes, is recommended. Ultimately, advancing the mechanistic understanding and practical deployment of LAB-derived QS modulators will support a more sustainable and low-risk strategy for biofilm control in food systems.

Author contributions

Dimitra Kostoglou: methodology, investigation, formal analysis, data curation, visualization. Alexandra Vlachopoulou: investigation. Georgios Vafeiadis: investigation. Efstathios Giaouris: methodology, project administration, resources, formal analysis, data curation, visualization, writing – original draft; writing – review & editing, supervision, funding acquisition, conceptualization.

Conflicts of interest

The authors declare no conflict of interest.

Data availability

Data can be provided upon reasonable request.

Supplementary information (SI): Table S1, Fig. S1 and S2. See DOI: <https://doi.org/10.1039/d5fb00384a>.

Acknowledgements

We thank Dr Nikolaos Chorianopoulos from the Agricultural University of Athens, Greece, for providing us with the two *V. harveyi* strains (BAA-1117 and BAA-1119) used in the luminescence-based QS assays. We also thank Dr Nikolaos Andritsos from Athens Analysis Laboratories S.A., Metamorfosi, Greece, for providing us with the *L. monocytogenes* AAL 20107 strain. We also acknowledge Dr Anagnostis Argyriou and his team for identifying some specific LAB isolates through 16S rRNA Sanger sequencing at the Institute of Applied Biosciences at the Centre for Research and Technology Hellas in Thessaloniki, Greece. This project was carried out within the framework of the National Recovery and Resilience Plan Greece 2.0, funded by the European Union—NextGenerationEU (Implementation body: Hellenic Foundation for Research and Innovation, HFRI; Project: “Combating biofilms of foodborne bacterial pathogens through a novel biocontrol approach employing lactic acid bacteria (LAB) postbiotics as modulators of cell-to-cell communication”; Project No. 15572). During the preparation of this work, the authors used ChatGPT to improve the language quality and readability. After using this tool, the



authors reviewed and edited the content as needed and take full responsibility for the content of the publication.

References

- 1 M. Gallo, L. Ferrara, A. Calogero, D. Montesano and D. Naviglio, *Food Res. Int.*, 2020, **137**, 109414.
- 2 A. Alvarez-Ordóñez, V. Broussolle, P. Colin, C. Nguyen-The and M. Prieto, *Int. J. Food Microbiol.*, 2015, **213**, 99–109.
- 3 European Food Safety Authority (EFSA) and European Centre for Disease Prevention and Control (ECDC), *EFSA J.*, 2024, **22**, e9106.
- 4 A. C. Ribeiro, F. A. d. Almeida, M. M. Medeiros, B. R. Miranda, U. M. Pinto and V. F. Alves, *Dairy*, 2023, **4**, 316–344.
- 5 Z. Wang, X. Tao, S. Liu, Y. Zhao and X. Yang, *Infect. Drug Resist.*, 2021, **14**, 1967–1978.
- 6 J. V. D. S. Emiliano, A. Fusieger, A. C. Camargo, F. F. D. C. Rodrigues, L. A. Nero, Í. T. Perrone and A. F. Carvalho, *Foodborne Pathog. Dis.*, 2024, **21**, 601–616.
- 7 X. Liu, X. Xia, Y. Liu, Z. Li, T. Shi, H. Zhang and Q. Dong, *Food Res. Int.*, 2024, **180**, 114067.
- 8 A. C. Silva-de-Jesus, R. G. Ferrari, P. Panzenhagen and C. A. Conte-Junior, *Microbiology*, 2022, **168**, 10.
- 9 M. Sharan, D. Vijay, P. Dhaka, J. S. Bedi and J. P. S. Gill, *J. Appl. Microbiol.*, 2022, **133**, 2210–2234.
- 10 W. Yin, S. Xu, Y. Wang, Y. Zhang, S. H. Chou, M. Y. Galperin and J. He, *Crit. Rev. Microbiol.*, 2021, **47**, 57–78.
- 11 A. Alvarez-Ordóñez, L. M. Coughlan, R. Briandet and P. D. Cotter, *Annu. Rev. Food Sci. Technol.*, 2019, **10**, 173–195.
- 12 X. Bai, C. H. Nakatsu and A. K. Bhunia, *Foods*, 2021, **10**, 2117.
- 13 M. Elaffify, X. Liao, J. Feng, J. Ahn and T. Ding, *Food Res. Int.*, 2024, **190**, 114650.
- 14 X. Zeng, Y. Zou, J. Zheng, S. Qiu, L. Liu and C. Wei, *Microbiol. Res.*, 2023, **273**, 127414.
- 15 J. Zhao, C. Quan, L. Jin and M. Chen, *J. Biotechnol.*, 2018, **268**, 53–60.
- 16 M. Tonkin, S. Khan, M. Y. Wani and A. Ahmad, *Curr. Pharm. Des.*, 2021, **27**, 2835–2847.
- 17 Y. Wang, Z. Bian and Y. Wang, *Appl. Microbiol. Biotechnol.*, 2022, **106**, 6365–6381.
- 18 S. Mukherjee and B. L. Bassler, *Nat. Rev. Microbiol.*, 2019, **17**, 371–382.
- 19 J. Li and X. Zhao, *Food Res. Int.*, 2020, **137**, 109742.
- 20 I. Machado, L. R. Silva, E. D. Giaouris, L. F. Melo and M. Simões, *Food Res. Int.*, 2020, **127**, 108754.
- 21 J. Fu, Y. Zhang, S. Lin, W. Zhang, G. Shu, J. Lin, H. Li, F. Xu, H. Tang, G. Peng, L. Zhao, S. Chen and H. Fu, *Front. Microbiol.*, 2021, **12**, 675843.
- 22 R. Roy, M. Tiwari, G. Donelli and V. Tiwari, *Virulence*, 2018, **9**, 522–554.
- 23 S. Challan Belval, L. Gal, S. Margiewes, D. Garmyn, P. Piveteau and J. Guzzo, *Appl. Environ. Microbiol.*, 2006, **72**, 2644–2650.
- 24 S. Sela, S. Frank, E. Belausov and R. Pinto, *Appl. Environ. Microbiol.*, 2006, **72**, 5653–5658.
- 25 R. Ma, S. Qiu, Q. Jiang, H. Sun, T. Xue, G. Cai and B. Sun, *Int. J. Med. Microbiol.*, 2017, **307**, 257–267.
- 26 K. Schilcher and A. R. Horswill, *Microbiol. Mol. Biol. Rev.*, 2020, **84**, e00026–19.
- 27 A. Zapaśnik, B. Sokołowska and M. Bryła, *Foods*, 2022, **11**, 1283.
- 28 F. De Filippis, E. Pasolli and D. Ercolini, *FEMS Microbiol. Rev.*, 2020, **44**, 454–489.
- 29 F. Meng, M. Zhao and Z. Lu, *Trends Food Sci. Technol.*, 2022, **127**, 272–279.
- 30 E. Giaouris, *Recent Trends Biofilm Sci. Technol.*, Academic Press, Elsevier Inc., London, 2020, pp. 205–232.
- 31 M. A. Díaz, E. G. Vega-Hissi, M. A. Blázquez, M. R. Alberto and M. E. Arena, *Antibiotics*, 2024, **13**, 297.
- 32 M. E. Kiyimaci, N. Altanlar, M. Gumustas, S. A. Ozkan and A. Akin, *Microb. Pathog.*, 2018, **121**, 190–197.
- 33 P. H. Marques, A. K. Jaiswal, F. A. de Almeida, U. M. Pinto, A. B. Ferreira-Machado, S. Tiwari, S. C. Soares and A. D. Paiva, *Mol. Diversity*, 2024, **28**, 2897–2912.
- 34 W. Pelyuntha, C. Chaiyasut, D. Kantachote and S. Sirilun, *PeerJ*, 2019, **7**, e7555.
- 35 S. Rana, S. Bhawal, A. Kumari, S. Kapila and R. Kapila, *Microb. Pathog.*, 2020, **142**, 104105.
- 36 R. Wasfi, O. A. Abd El-Rahman, M. M. Zafer and H. M. Ashour, *J. Cell. Mol. Med.*, 2018, **22**, 1972–1983.
- 37 I. S. Rotta, S. D. D. C. Rezende, H. F. Perini, M. V. da Silva, F. A. de Almeida, U. M. Pinto, A. B. Ferreira Machado and A. D. Paiva, *Front. Microbiol.*, 2025, **16**, 1601203.
- 38 Z. Deng, K. Hou, T. G. Valencak, X. M. Luo, J. Liu and H. Wang, *Microbiol. Spectrum*, 2022, **10**, e0061022.
- 39 Y. Qian, C. Zhao, X. Cai, M. Zeng and Z. Liu, *Int. J. Food Microbiol.*, 2023, **389**, 110102.
- 40 X. Wang, X. Li and J. Ling, *J. Basic Microbiol.*, 2017, **57**, 605–616.
- 41 L. Xiao, Q. An, R. Xu, C. Li, C. Zhang, K. Ma, F. Ji, E. Azarpazhooh, M. Ajami, X. Rui and W. Li, *Microb. Pathog.*, 2023, **184**, 106379.
- 42 S. A. McEwen and P. J. Collignon, *Microbiol. Spectrum*, 2018, **6**, DOI: [10.1128/microbiolspec.arba-0009-2017](https://doi.org/10.1128/microbiolspec.arba-0009-2017).
- 43 A. Meireles, E. Giaouris and M. Simões, *Food Res. Int.*, 2016, **82**, 71–85.
- 44 E. Paluch, J. Rewak-Soroczyńska, I. Jędrusik, E. Mazurkiewicz and K. Jermakow, *Appl. Microbiol. Biotechnol.*, 2020, **104**, 1871–1881.
- 45 M. Despotovic, L. de Nies, S. B. Busi and P. Wilmes, *Curr. Opin. Microbiol.*, 2023, **73**, 102291.
- 46 G. Zoumpopoulou, K. Papadimitriou, V. Alexandraki, E. Mavrogonatou, K. Alexopoulou, R. Anastasiou, M. Georgalaki, D. Kletsas, E. Tsakalidou and E. Giaouris, *LWT–Food Sci. Technol.*, 2020, **130**, 109570.
- 47 B. L. Bassler, E. P. Greenberg and A. M. Stevens, *J. Bacteriol.*, 1997, **179**, 4043–4045.
- 48 L. Lu, M. E. Hume and S. D. Pillai, *J. Food Prot.*, 2004, **67**, 1457–1462.
- 49 M. G. Surette and B. L. Bassler, *Proc. Natl. Acad. Sci. U. S. A.*, 1998, **95**, 7046–7050.



- 50 D. Vetas, E. Dimitropoulou, G. Mitropoulou, Y. Kourkoutas and E. Giaouris, *Int. J. Food Microbiol.*, 2017, **257**, 19–25.
- 51 J. Baranyi and T. A. Roberts, *Int. J. Food Microbiol.*, 1994, **23**, 277–294.
- 52 V. A. Blana, A. I. Doulgeraki and G. J. Nychas, *J. Food Prot.*, 2011, **74**, 631–635.
- 53 H. Park, H. Shin, K. Lee and W. Holzapfel, *Int. J. Food Microbiol.*, 2016, **225**, 38–42.
- 54 J. C. Augustin, L. Rosso and V. Carlier, *J. Microbiol. Methods*, 1999, **38**, 137–146.
- 55 P. Dalgaard and K. Koutsoumanis, *J. Microbiol. Methods*, 2001, **43**, 183–196.
- 56 P. Dalgaard, T. Ross, L. Kamperman, K. Neumeyer and T. A. McMeekin, *Int. J. Food Microbiol.*, 1994, **23**, 391–404.
- 57 D. Kostoglou, A. Vass and E. Giaouris, *Antibiotics*, 2024, **13**, 201.
- 58 D. Strantzali, D. Kostoglou, A. Perikleous, M. Zestas, S. Ornithopoulou, F. Dubois-Brissonnet and E. Giaouris, *Food Control*, 2021, **129**, 108239.
- 59 H. Park, S. Yeo, Y. Ji, J. Lee, J. Yang, S. Park, H. Shin and W. Holzapfel, *Food Control*, 2014, **45**, 62–69.
- 60 M. I. Hossain, M. F. R. Mizan, P. K. Roy, S. Nahar, S. H. Tousehik, M. Ashrafudoulla, I. K. Jahid, J. Lee and S. D. Ha, *Food Res. Int.*, 2021, **148**, 110595.
- 61 Y. Liang, Y. Pan, Q. Li, B. Wu and M. Hu, *Int. Microbiol.*, 2022, **25**, 447–456.
- 62 M. J. Medellin-Peña and M. W. Griffiths, *Appl. Environ. Microbiol.*, 2009, **75**, 1165–1172.
- 63 A. S. Okamoto, R. L. Andreatti Filho, E. L. Milbradt, A. C. I. Moraes, I. H. B. Vellano and P. T. C. Guimarães-Okamoto, *Poult. Sci.*, 2018, **97**, 2708–2712.
- 64 J. Li, X. Yang, G. Shi, J. Chang, Z. Liu and M. Zeng, *Food Res. Int.*, 2019, **120**, 679–687.
- 65 Y. J. Lee and C. Wang, *MicrobiologyOpen*, 2020, **9**, e1015.
- 66 C. U. Riedel, I. R. Monk, P. G. Casey, M. S. Waidmann, C. G. Gahan and C. Hill, *Mol. Microbiol.*, 2009, **71**, 1177–1189.
- 67 D. Yu, L. Zhao, T. Xue and B. Sun, *BMC Microbiol.*, 2012, **12**, 288.
- 68 J. Lee, J. Park, J. Baek, S. Lee, E. Seo, S. Kim, H. Choi and S. S. Kang, *Int. J. Food Microbiol.*, 2025, **430**, 111066.
- 69 C. Melian, F. Segli, R. Gonzalez, G. Vignolo and P. Castellano, *J. Appl. Microbiol.*, 2019, **127**, 911–920.
- 70 J. Wei, X. Zhang, M. Ismael and Q. Zhong, *Foods*, 2024, **13**, 2495.
- 71 J. Liu, W. Li, X. Zhu, H. Zhao, Y. Lu, C. Zhang and Z. Lu, *Appl. Microbiol. Biotechnol.*, 2019, **103**, 4565–4574.
- 72 N. Doherty, M. T. Holden, S. N. Qazi, P. Williams and K. Winzer, *J. Bacteriol.*, 2006, **188**, 2885–2897.
- 73 M. Hurtová, K. Káňová, S. Dobiasová, K. Holasová, D. Čáková, L. Hoang, D. Biedermann, M. Kuzma, J. Cvačka, V. Křen, J. Viktorová and K. Valentová, *Int. J. Mol. Sci.*, 2022, **23**, 15121.
- 74 Y. Mao, P. Liu, H. Chen, Y. Wang, C. Li and Q. Wang, *Infect. Drug Resist.*, 2023, **16**, 2861–2882.
- 75 G. Milli, A. Pellegrini, R. Listro, M. Fasolini, K. Pagano, L. Ragona, G. Pietrocola, P. Linciano and S. Collina, *J. Med. Chem.*, 2024, **67**, 18139–18156.
- 76 F. Sedlmayer, A. K. Woischnig, V. Unterreiner, F. Fuchs, D. Baeschlin, N. Khanna and M. Fussenegger, *Nucleic Acids Res.*, 2021, **49**, e73.
- 77 X. Yan, S. Gu, X. Cui, Y. Shi, S. Wen, H. Chen and J. Ge, *Microb. Pathog.*, 2019, **127**, 12–20.
- 78 Y. Zhang, L. Dong, L. Sun, X. Hu, X. Wang, T. Nie, X. Li, P. Wang, P. Pang, J. Pang, X. Lu, K. Yao and X. You, *Front. Microbiol.*, 2022, **13**, 980217.

